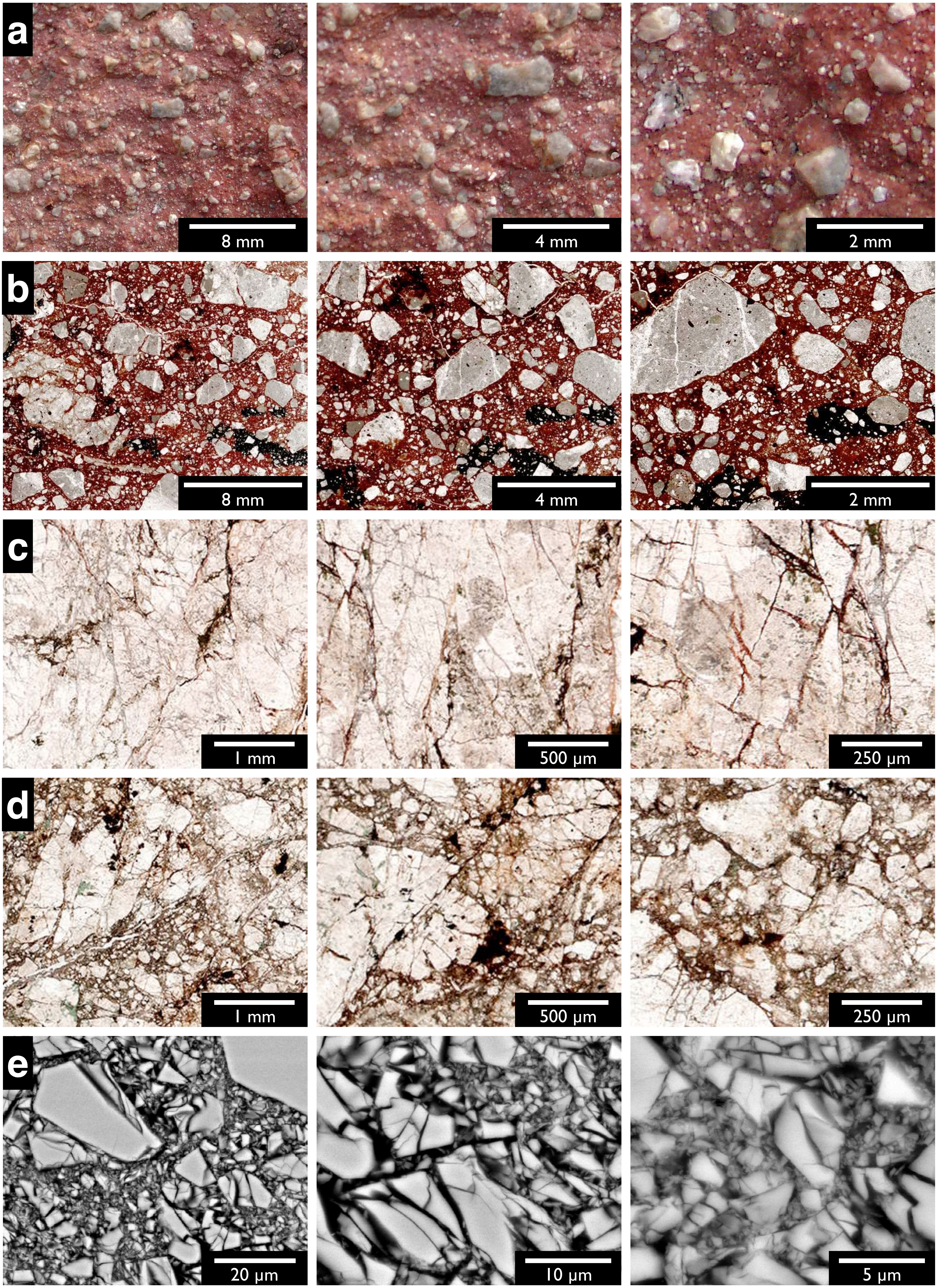

Figure 13.1

Self-similarity at various scales

Various types of fault rock, shown at increasing magnifications:

(a) shown in outcrop; (b) same as (a) in thin section; (c) thin section with angular (in-situ) fragments; (d) same as (c) with angular (in-situ) and rounded (dislocated) fragments; (e) SEM micrograph with (dislocated) angular fragments.

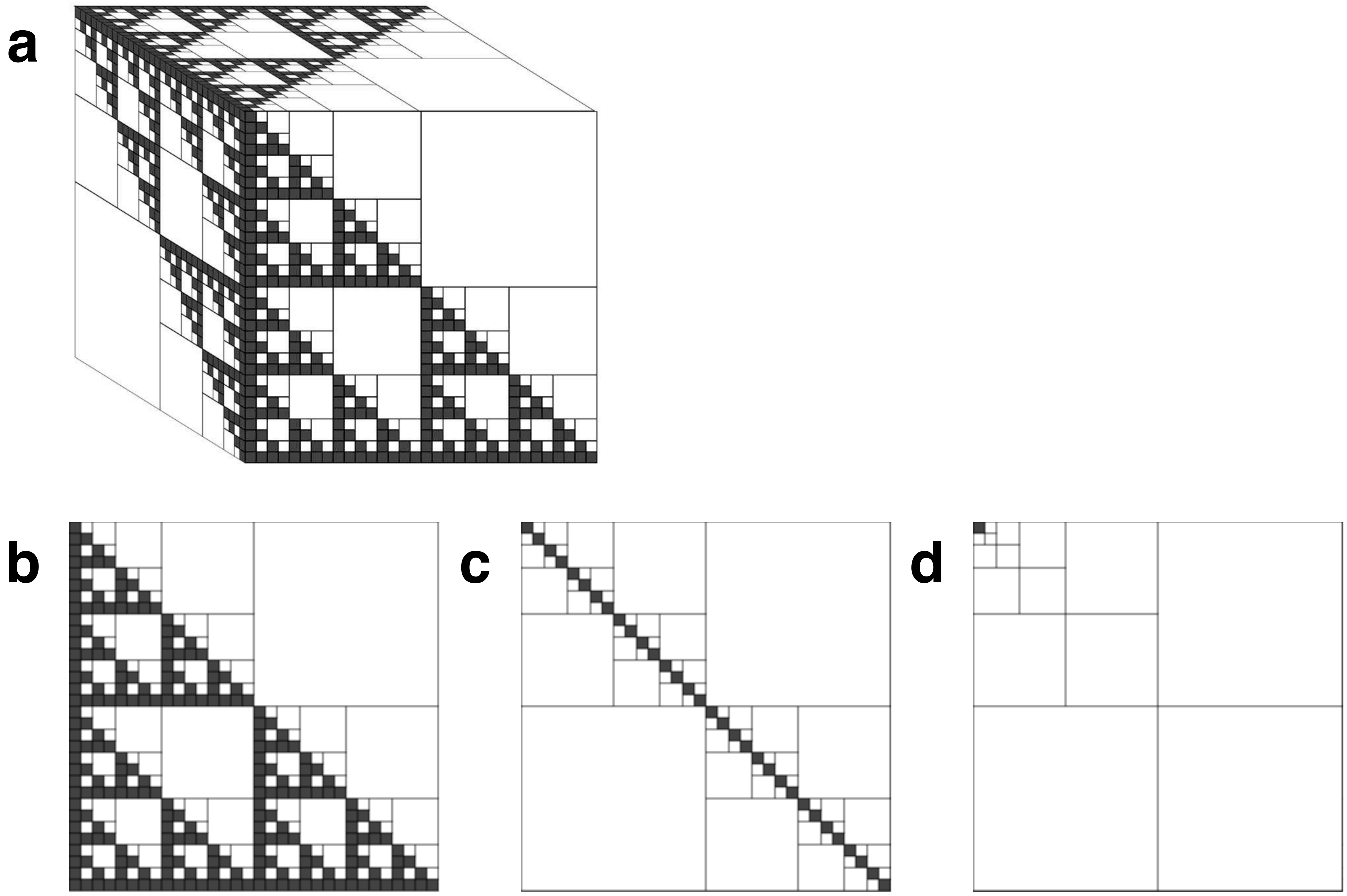

Figure 13.2
Fragmentation of a cube.
Fragmentation of the cube produces 8 cubes (F = 8) of 1/2 the width of the original.
(a) Example of a cube where, at each scale, 2 out of 8 cubes remain unfragmented (N = 2), while 6 are fragmented further;
(b) front view of cube (a): the fragmentation fraction, f = (F - N) / F = 6 / 8;
(c) front view of a cube with f = 4 / 8;
(d) front view of a cube with f = 1 / 8.

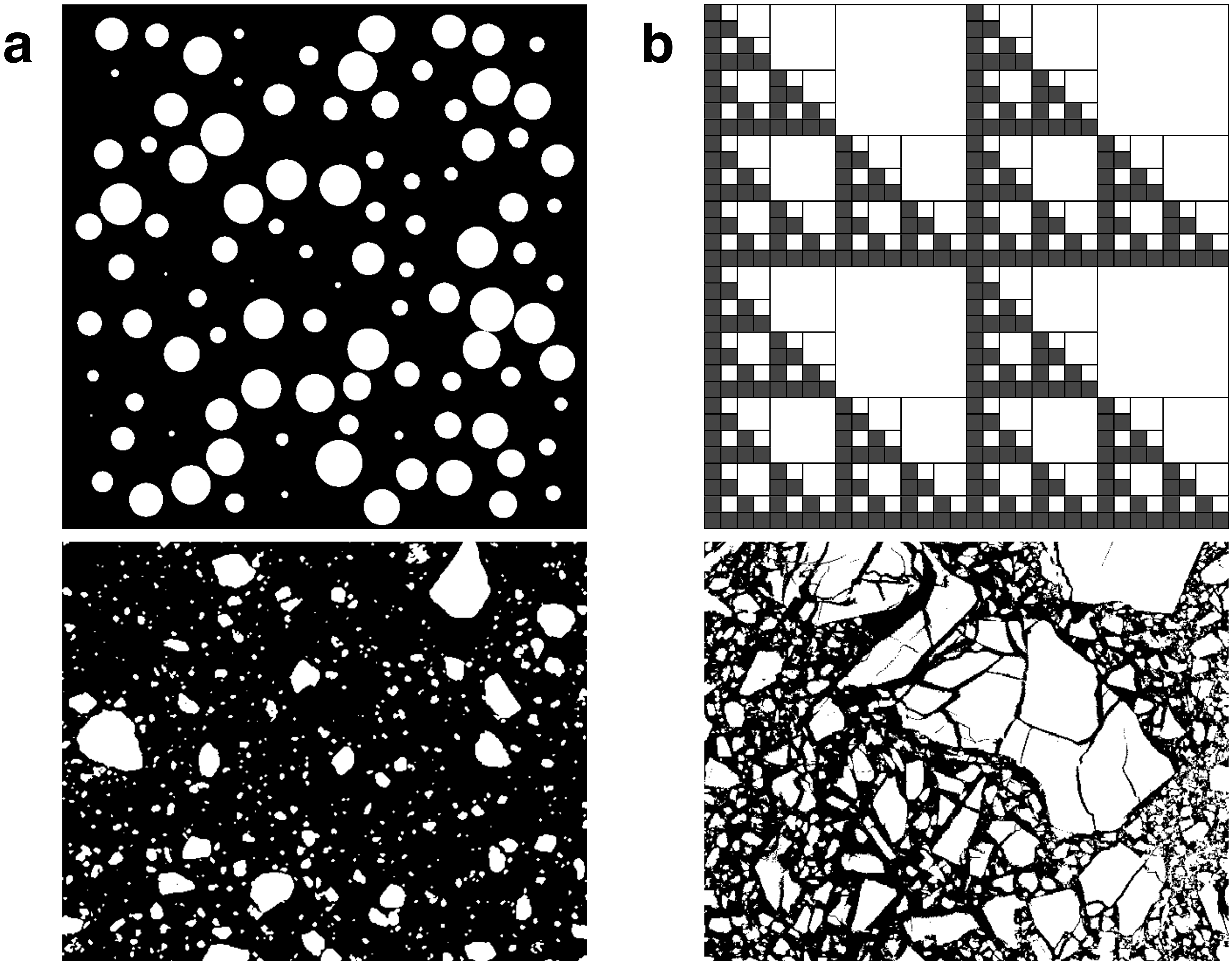

Figure 13.3
Two conceptual models for grain size determination.
(a) Stereological model: particles are diluted in matrix;
(b) fractal model: fragments are densely packed.

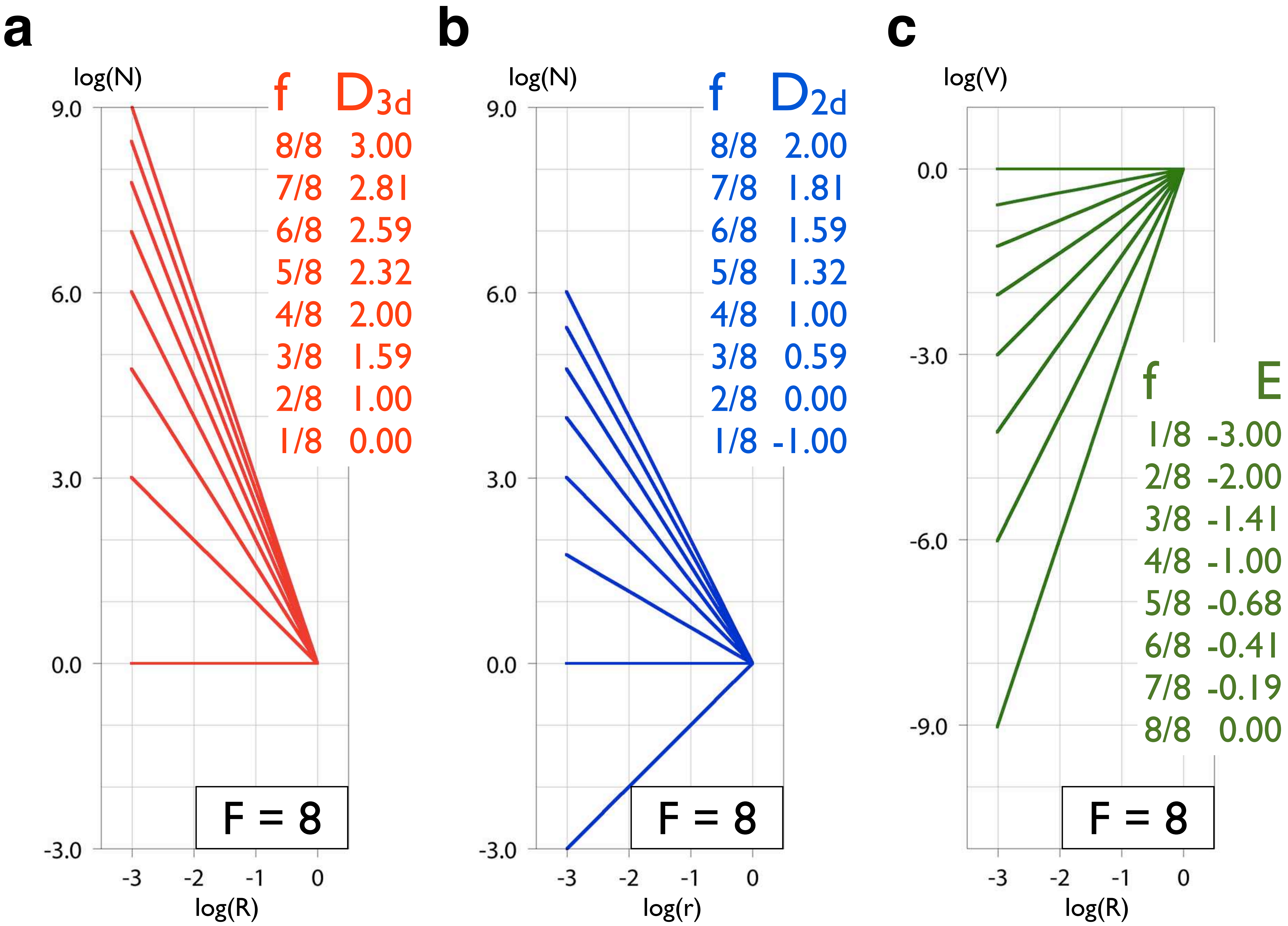

Figure 13.4
Fractal dimension of grain size distribution created by fragmenting a cube.
Fragmentation number, F, is 8 (as in Figure 13.2), fragmentation fractions, f, range from 1/8 to 7/8.
(a) Log(N)-log(r) plot, where N = number and R = size of fragments, the slope, D_{3d}, is the fractal dimension of the size distribution of 3-D grains;
(b) log(N)-log(r) plot where N = number and r = size of cross sections of fragments, the slope, D_{2d}, is the fractal dimension of the size distribution of 2-D grains;
(c) log(V)-log(r) plot where V = volume and R = size of fragments, $E = D_{3d} - 3$.

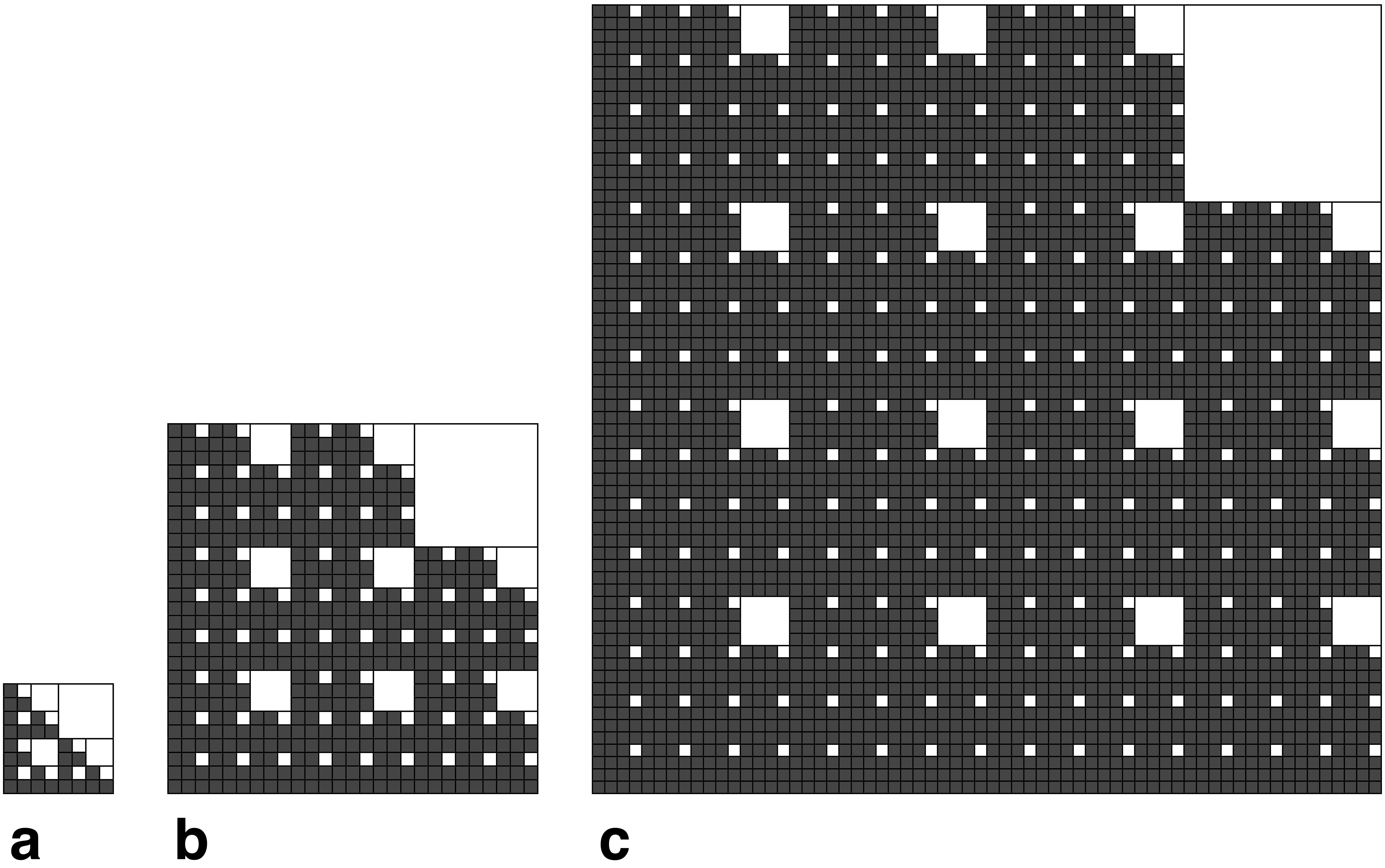

Figure 13.5
Higher fragmentation numbers.
Front views of cubes with different fragmentation numbers, F, and different fragmentation fractions, f.
The cube is fragmented into:
(a) $F = 2 \cdot 2 \cdot 2 = 8$, $N = 2$, $f = 6 / 8$;
(b) $F = 3 \cdot 3 \cdot 3 = 27$, $N = 3$, $f = 24 / 27$;
(c) $F = 4 \cdot 4 \cdot 4 = 64$, $N = 4$, $f = 60 / 64$.

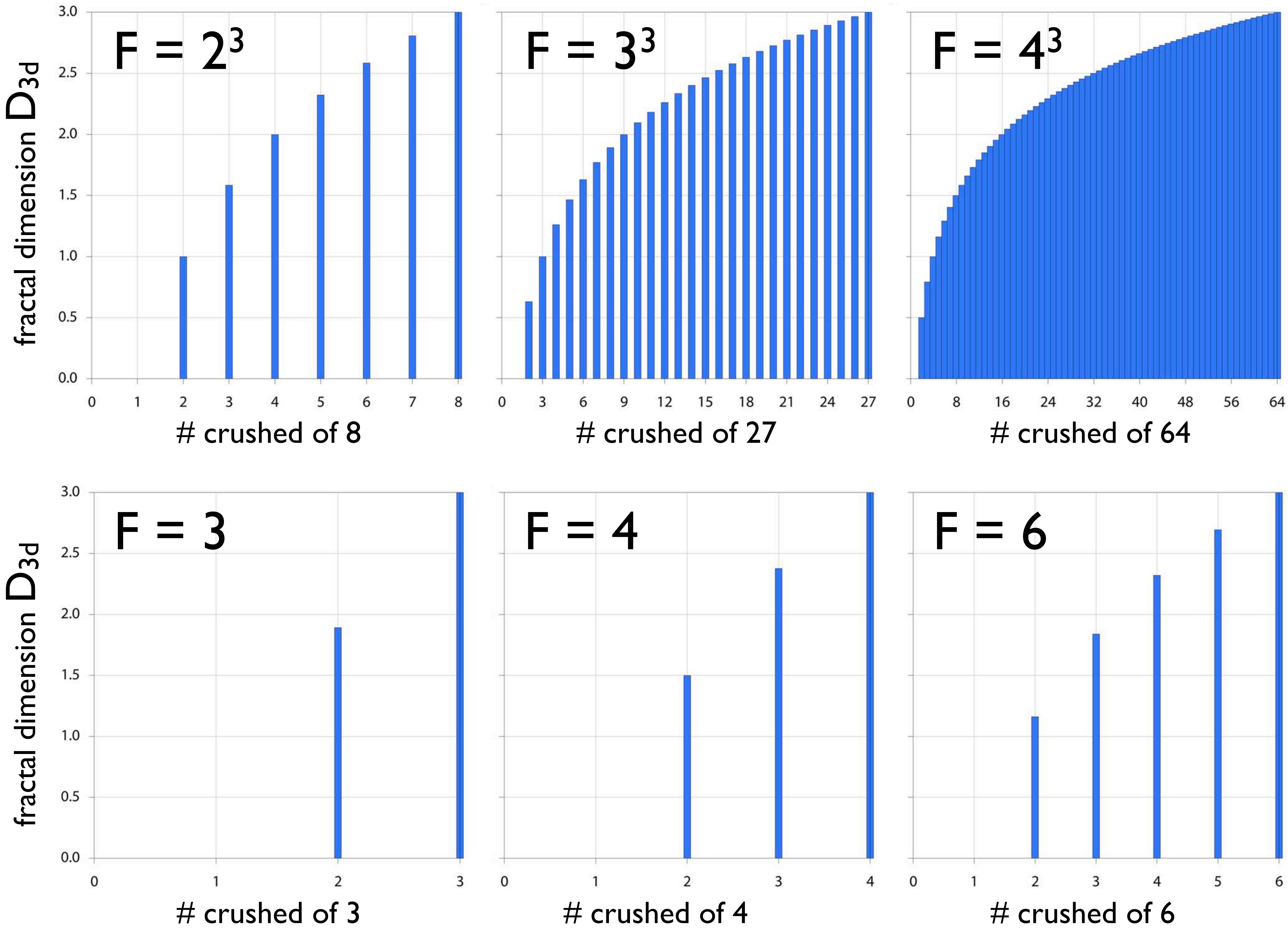

Figure 13.6
Fractal dimensions for different fragmentations.
Plots of fractal dimension, D_{3d}, versus number of crushed fragments, for different fragmentation numbers, F.

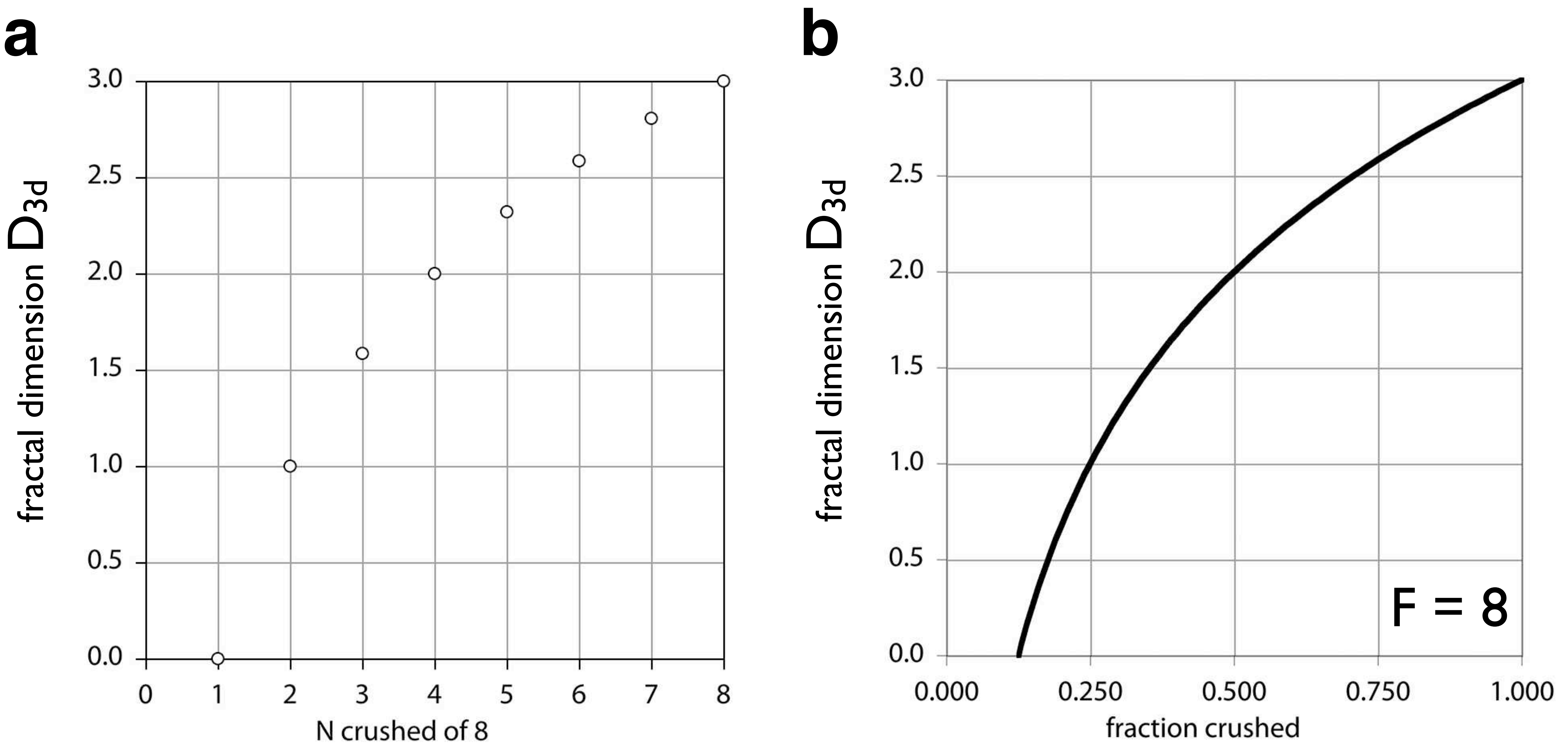

Figure 13.7
Fractal dimension for continuous fragmentation fraction, f.
Fragmentation number, F = 8.
(a) Discrete fragmentation fraction, $f = (F - N_i) / F$ for i = 1 to 8;
(b) same plot as (a) for continuously defined f : $(0.00 \leq f \leq 1.00)$.

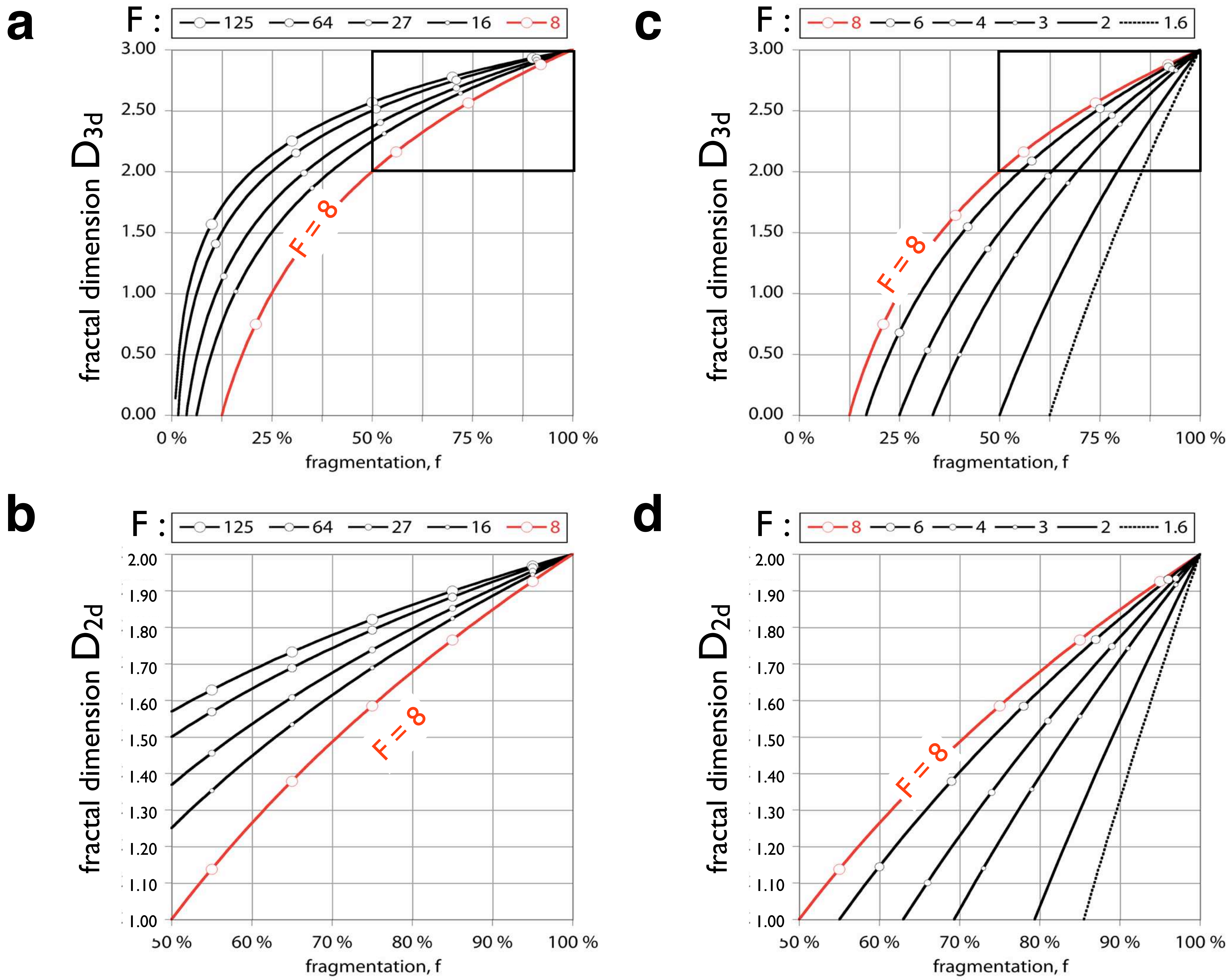

Figure 13.8
Fractal dimension for continuously defined fragmentation numbers and fragmentation fractions.
(a) D_{3d} for fragmentation numbers $F \geq 8$;
(b) D_{3d} for fragmentation numbers $F \leq 8$;
(c) D_{2d} for fragmentation numbers $F \geq 8$, note that $D_{2d} = D_{3d} - 1$;
(d) D_{2d} for fragmentation numbers $F \leq 8$, note that $D_{2d} = D_{3d} - 1$.
Plots (c) and (d) correspond to region framed in (a) and (b).

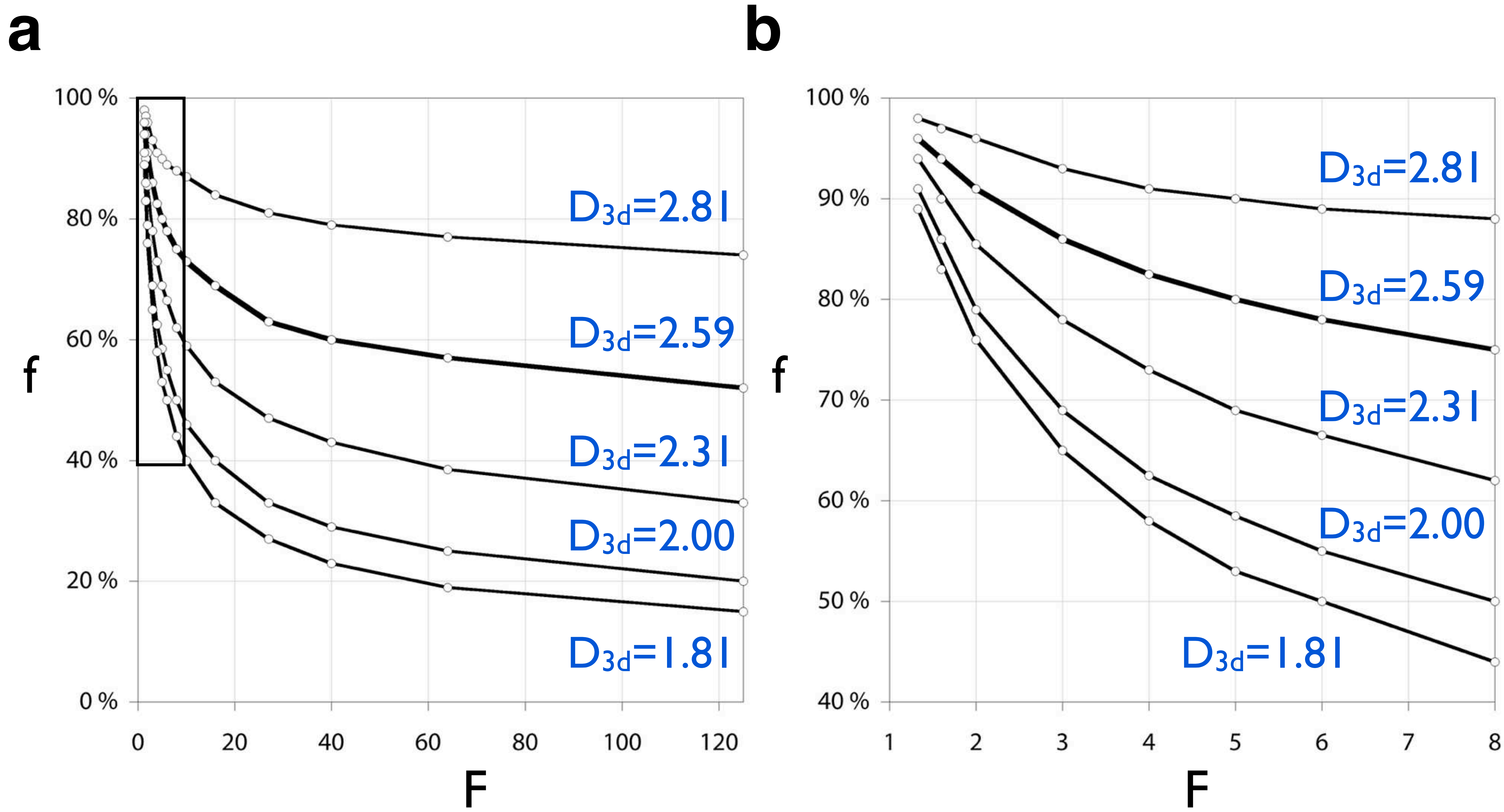

Figure 13.9
Fractal dimensions from different fragmentation processes.
Iso-lines of fractal dimension, D_{3d}, for varying fragmentation numbers, N, and fragmentation fractions, f.
(a) Curves of D_{3d} for ($0\% \leq f \leq 100\%$) and ($0 \leq F \leq 125$);
(b) expanded view of plot indicated by rectangle in (a) for ($50\% \leq f \leq 100\%$) and ($0 \leq F \leq 8$).

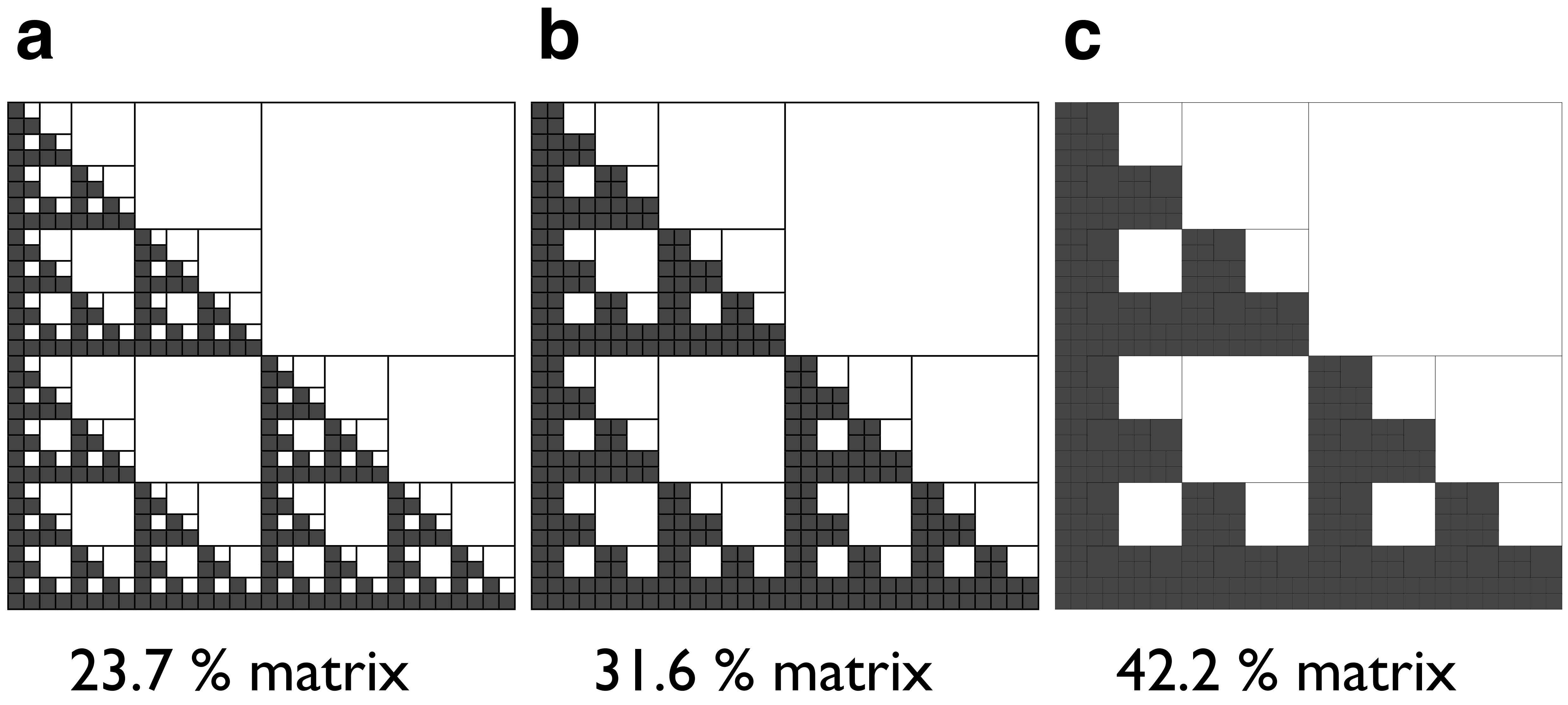

Figure 13.10
Concept of fragmentation matrix.
Area fraction of fragmentation matrix is defined by matrix length scale, L_m;
$L_m = g / G$ where g = largest grain in matrix and G = largest grain present in image.
(a) $L_m = 1 / 32$ and matrix content = 23.7 %;
(b) $L_m = 1 /16$ and matrix content = 31.6 %;
(c) $L_m = 1/ 8$ and matrix content = 42.2 %.

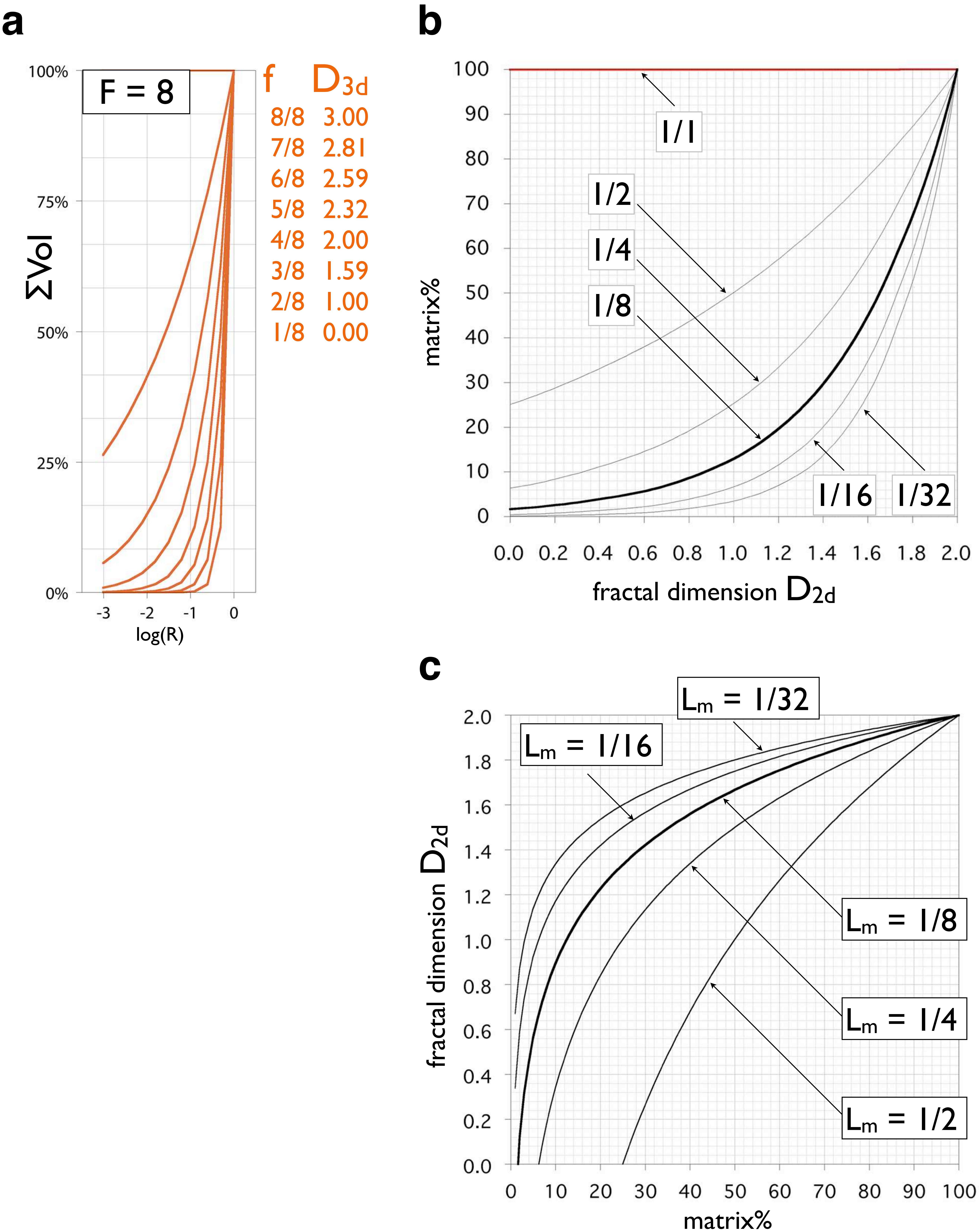

Figure 13.11
Apparent matrix content and fractal dimension.
(a) Cumulative volume, ΣV, is shown as function of log(R) for different D_{3d} (compare Figure 13.4.c); fragmentation number F = 8, f = fragmentation fraction, R = size of fragments, D_{3d} = fractal dimension of the size distribution of 3-D grains;
(b) matrix contents, m%, is shown as functions of D_{2d} for different matrix lengths scales, L_m; the fractal dimension ($0.00 \leq D_{2d} \leq 2.00$);
(c) matrix-D diagram showing fractal dimension ($0.00 \leq D_{2d} \leq 2.00$) versus matrix content for a range of matrix lengths scales, L_m = 1/32, 1/16, 1/8, 1/4 and 1/2 (for L_m see Figure 13.10).

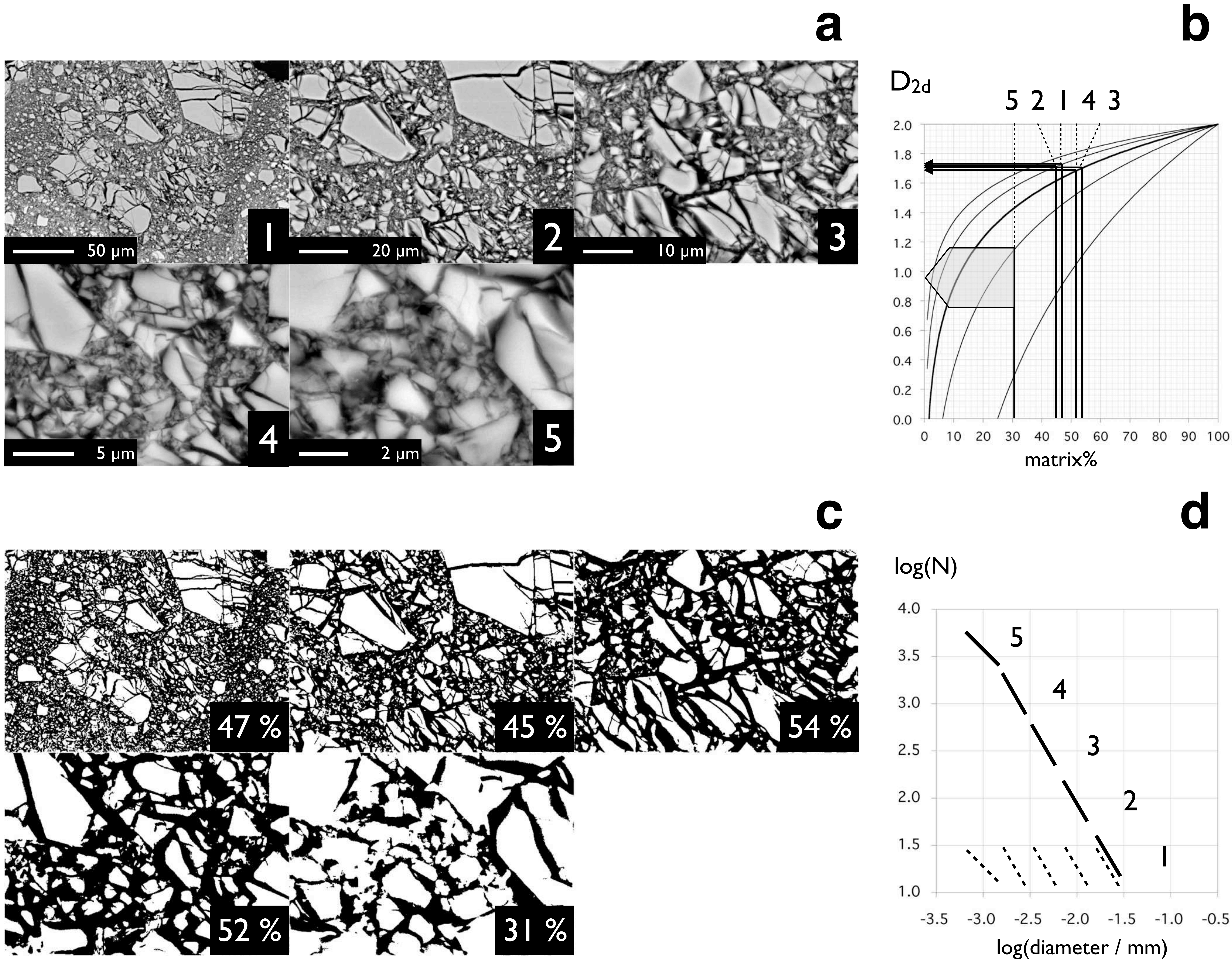

Figure 13.12
Deriving the fractal dimension from the matrix content.
(a) SEM micrograph of fault rock at increasing magnification;
(b) bitmaps of (a), area percentage of matrix indicated;
(c) matrix-D diagram (see Figure 13.11) with matrix data for samples 1 to 5; matrix length scale, L_m = 1/16 for 1,2, L_m = 1/8 for 3,4, and L_m > 1/4 for 5;
(d) log(N)-log(R) plot constructed from D-values (slopes) of areas 1 to 5.

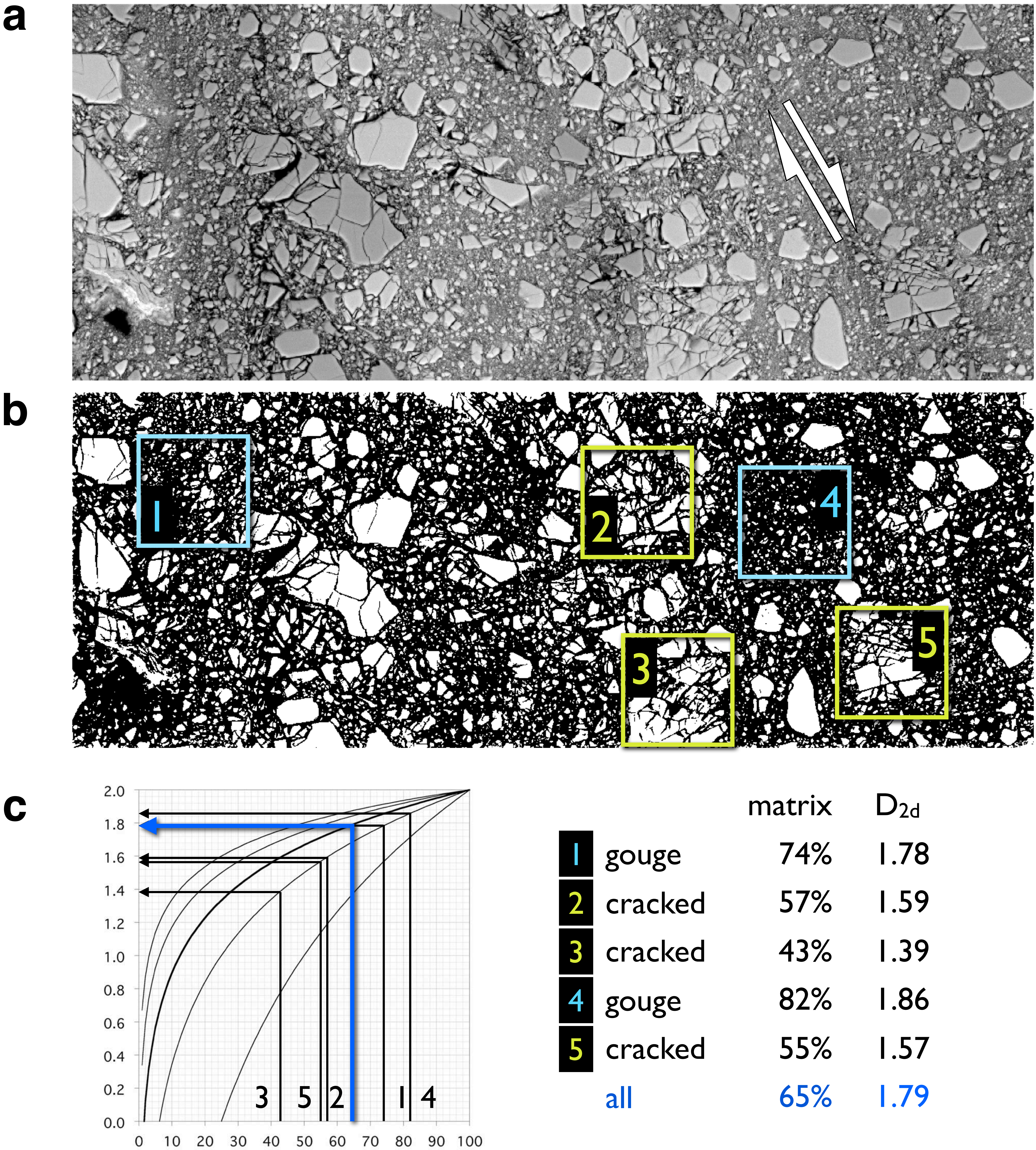

Figure 13.13
Local variation of the fractal dimension.
(a) SEM micrograph of experimentally produced cataclastic shear zone (displacement vertical, shear sense indicated, sample courtesy Nynke Keulen);
(b) bitmap of (a), 5 sites are indicated;
(c) matrix-D diagram (see Figure 13.11) with matrix data for sites 1 to 5; blue = data for entire bitmap; matrix length scale, L_m = 1/8 for entire image, L_m = 1/4 for areas 1 to 5.

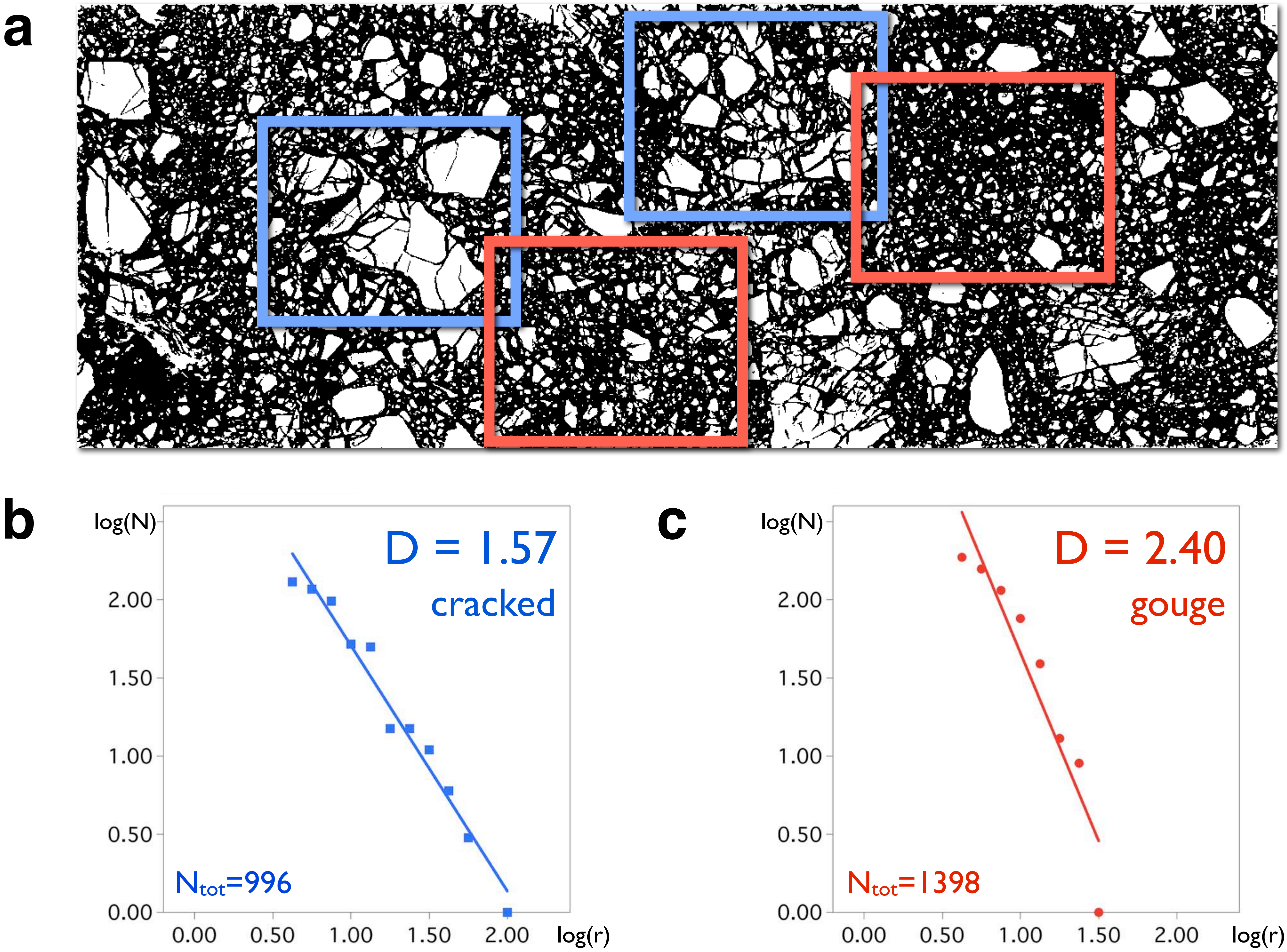

Figure 13.14
Non-fractal size distribution.
(a) Bitmap of experimentally produced cataclastic shear zone (Figure 13.13);
(b) grain size analysis of fragmented part;
(c) grain size analysis of part with mature gouge;
r = size, N = number of fragments, total number indicated; D = negative slope of line fit.

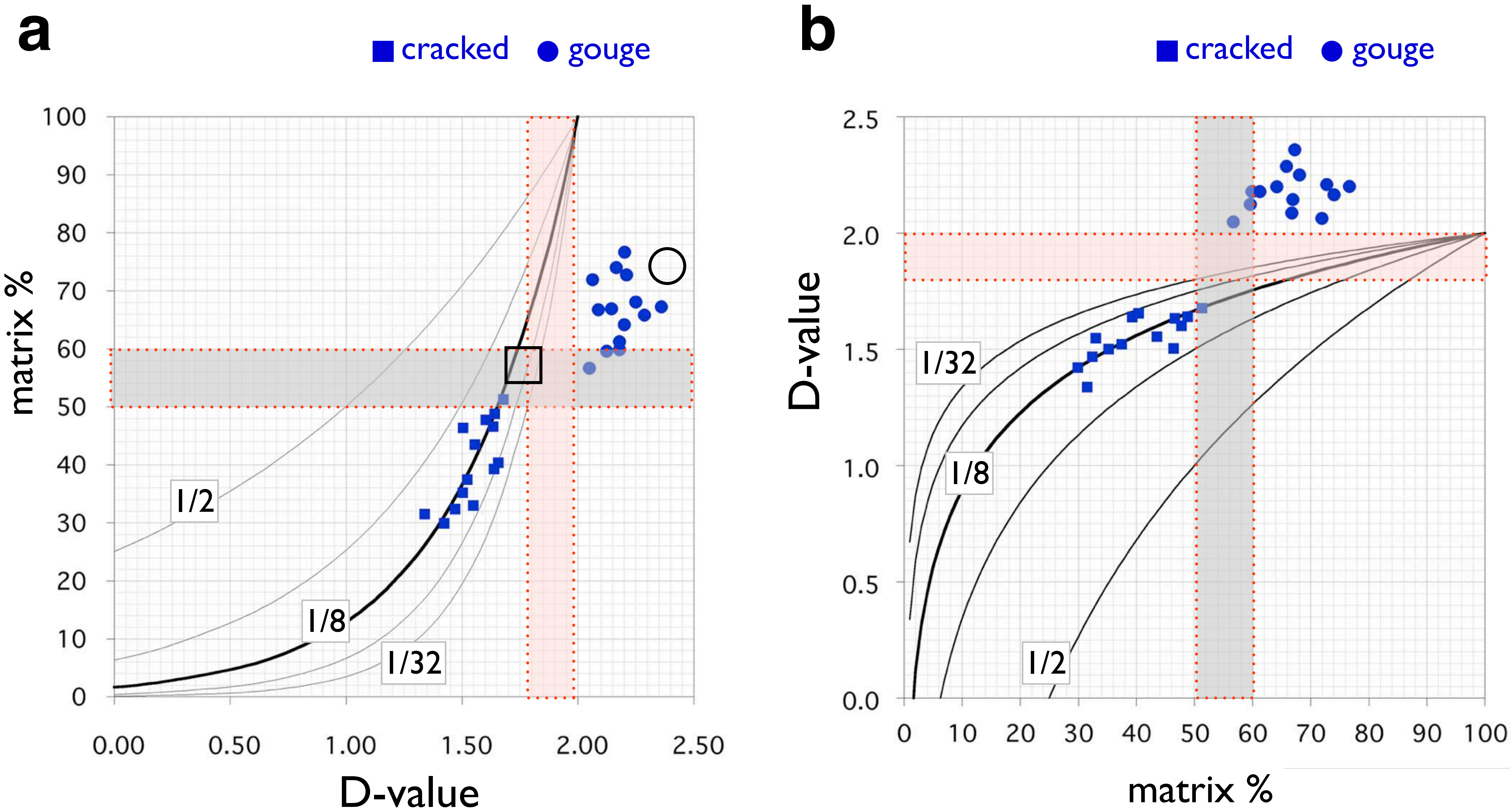

Figure 13.15
Fractal dimension from measured matrix content and D-value from measured grain size analysis.
(a) Matrix contents as functions of D, expanded version of plot shown in Figure 13.11.b; black symbols are measured data points for cracked and gouge material;
(b) expanded matrix-D diagram (see Figure 13.11.c); same data points as in Figure 13.15.a; note D > 2 for gouge.
Lines denote matrix lengths scales L_m = 1/32, 1/16, 1/8, 1/4 and 1/2 (see Figure 13.11.c);
pink and gray shaded areas outline range of matrix%- and D- values separating cracked from gouge material.

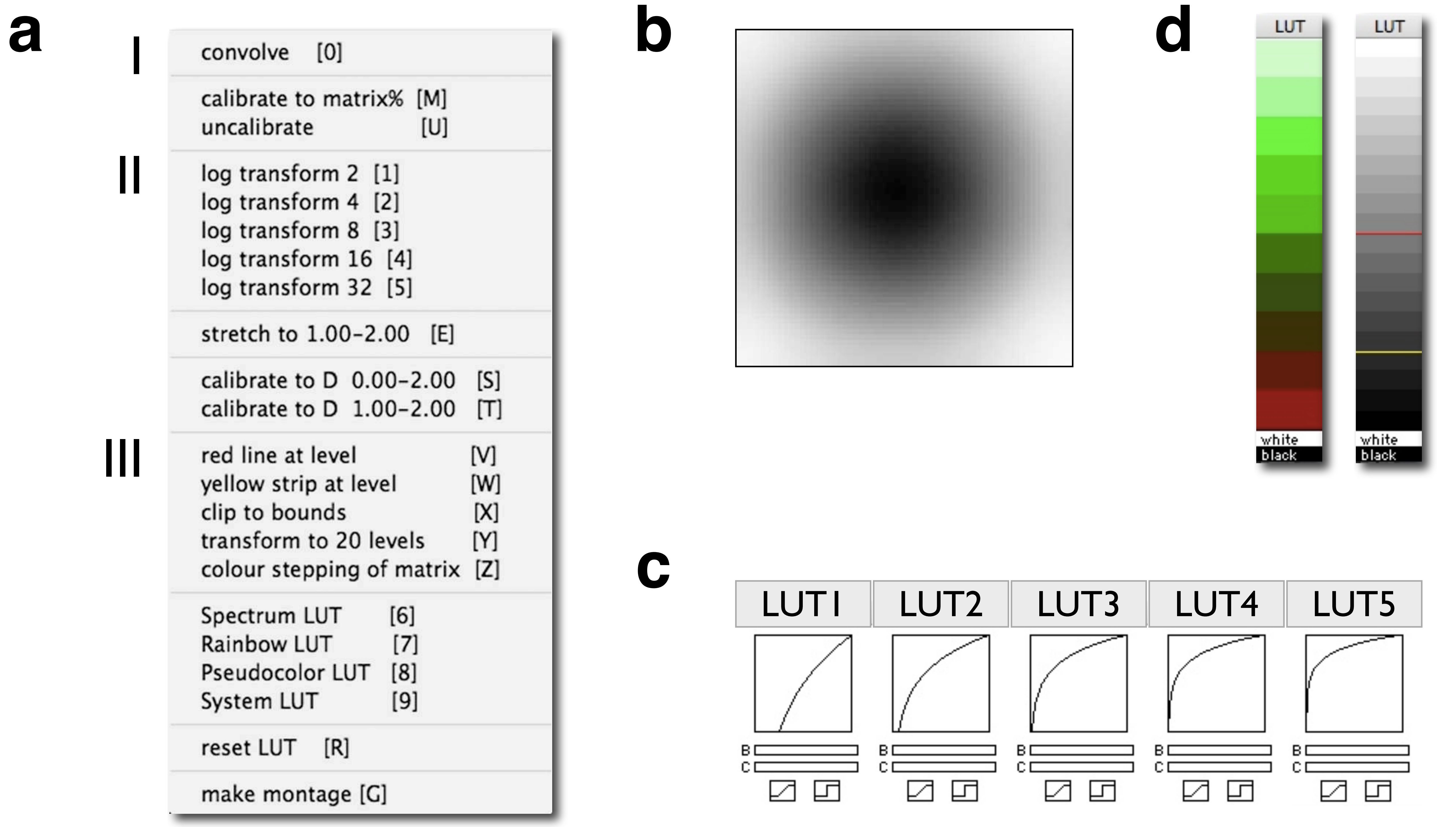

Figure 13.16
Mapping fractal dimensions of grain size distributions.
(a) The Lazy D map menu;
(b) step I: creating matrix density maps: 63 · 63 Gauss filter kernel shown as brightness image;
(c) step II: converting to fractal dimension: look-up tables LUT1 to LUT5 for matrix length scales, L_m, from 1/2 to 1/32
(d) step III: using color LUTs to visualize (example from left to right: 10 colors for 0-100% matrix, 20 steps with red line at 50% and yellow strip at 80%).

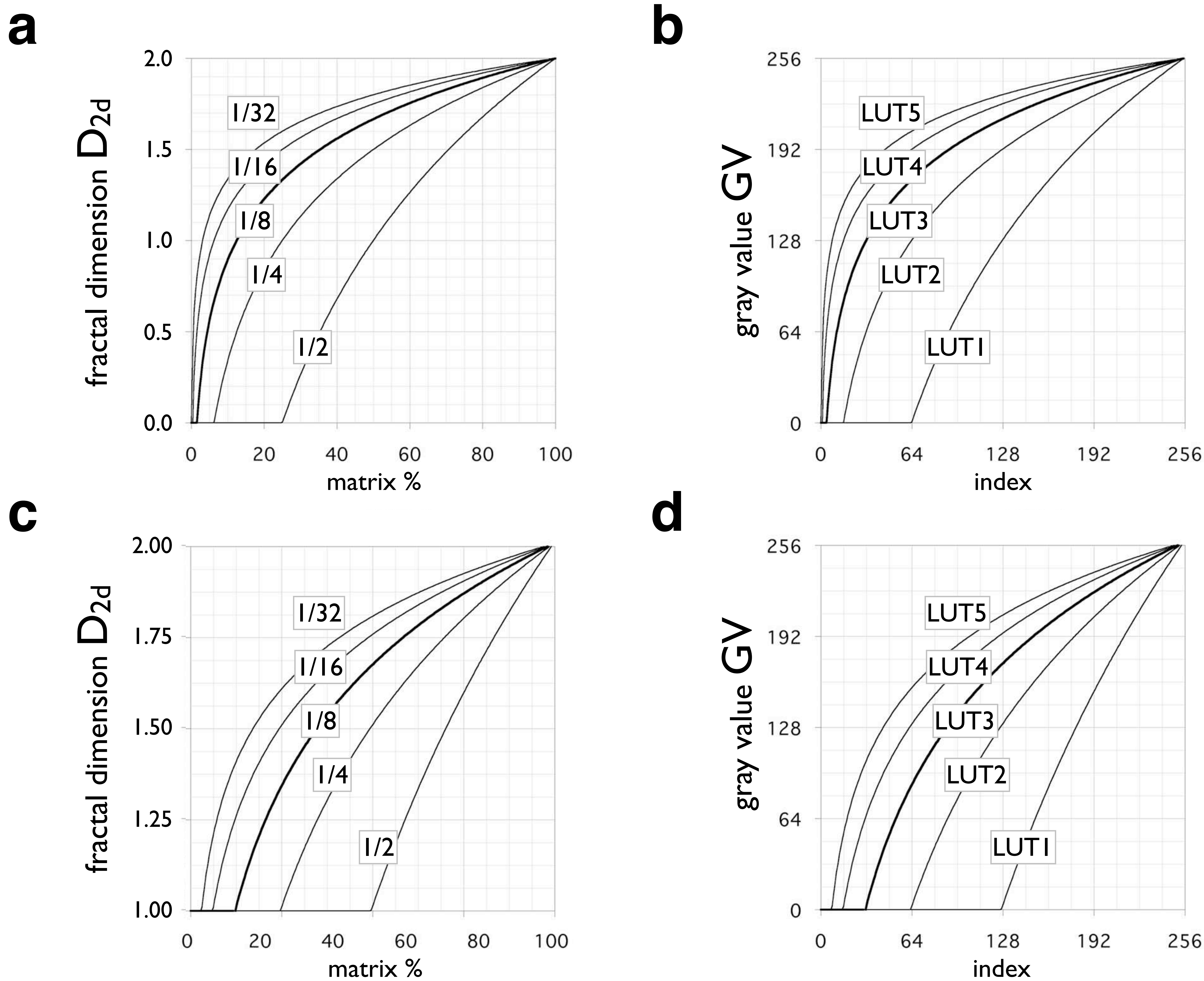

Figure 13.17
Creating look-up tables from matrix-D diagrams.
Matrix density (0% to 100%) is converted to index (0 to 255), fractal dimension, D_{2d}, to gray value, GV, (0 to 255).
(a) and (c) for ($0.00 \le D_{2d} \le 2.00$); matrix lengths scales, L_m, are indicated.
(b) and (d) for ($1.00 \le D_{2d} \le 2.00$); name of LUT indicated.

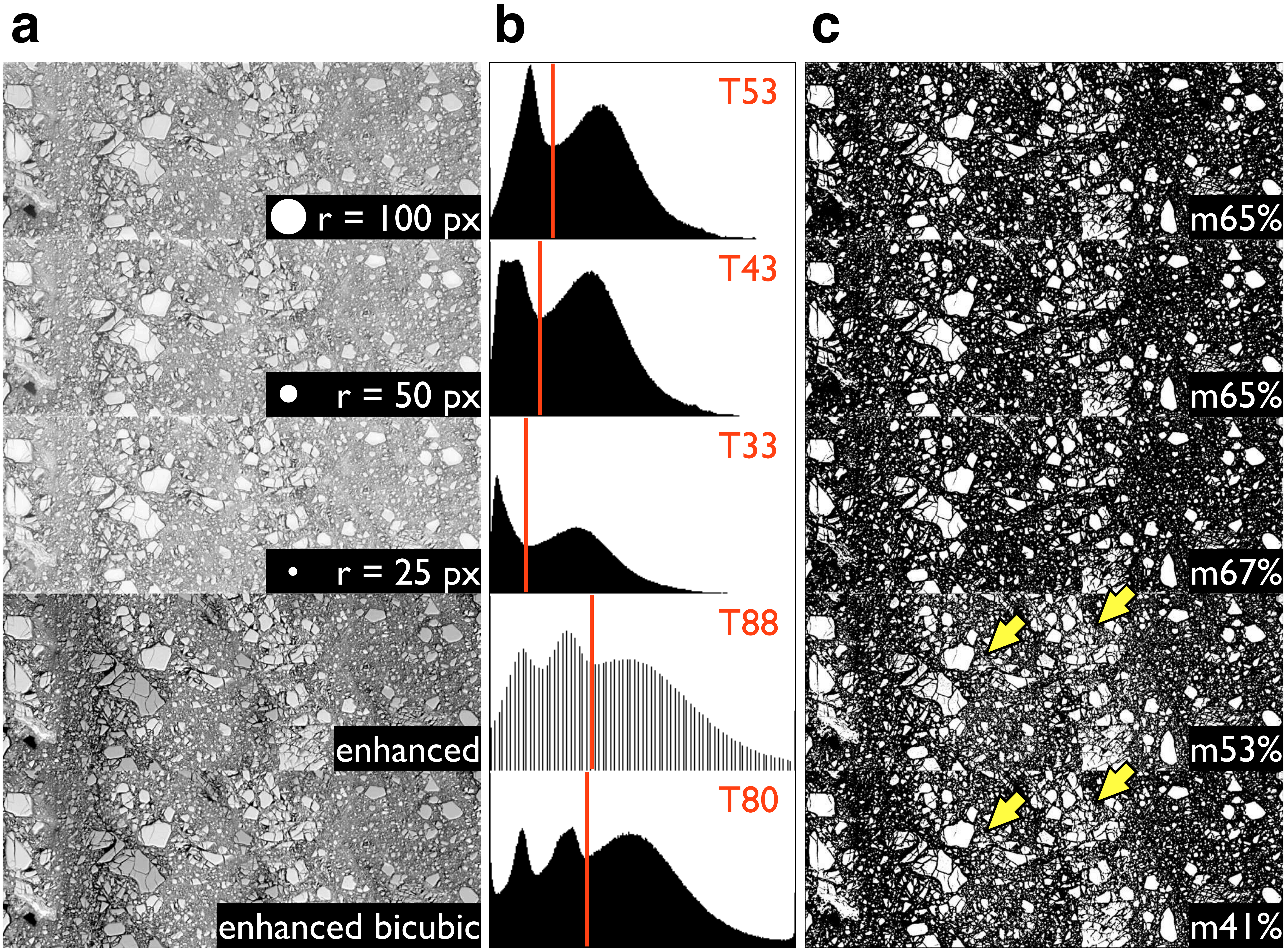

Figure 13.18
Preparing the bitmap.
Pre-processing by rolling ball background subtraction with decreasing radius, by enhancing, and bicubic smoothing (top to bottom).
(a) Grayscale images, radius of rolling ball indicated;
(b) histogram with threshold level indicated;
(c) resulting bitmap, average area fraction of matrix indicated; arrows point to areas where matrix is underestimated.

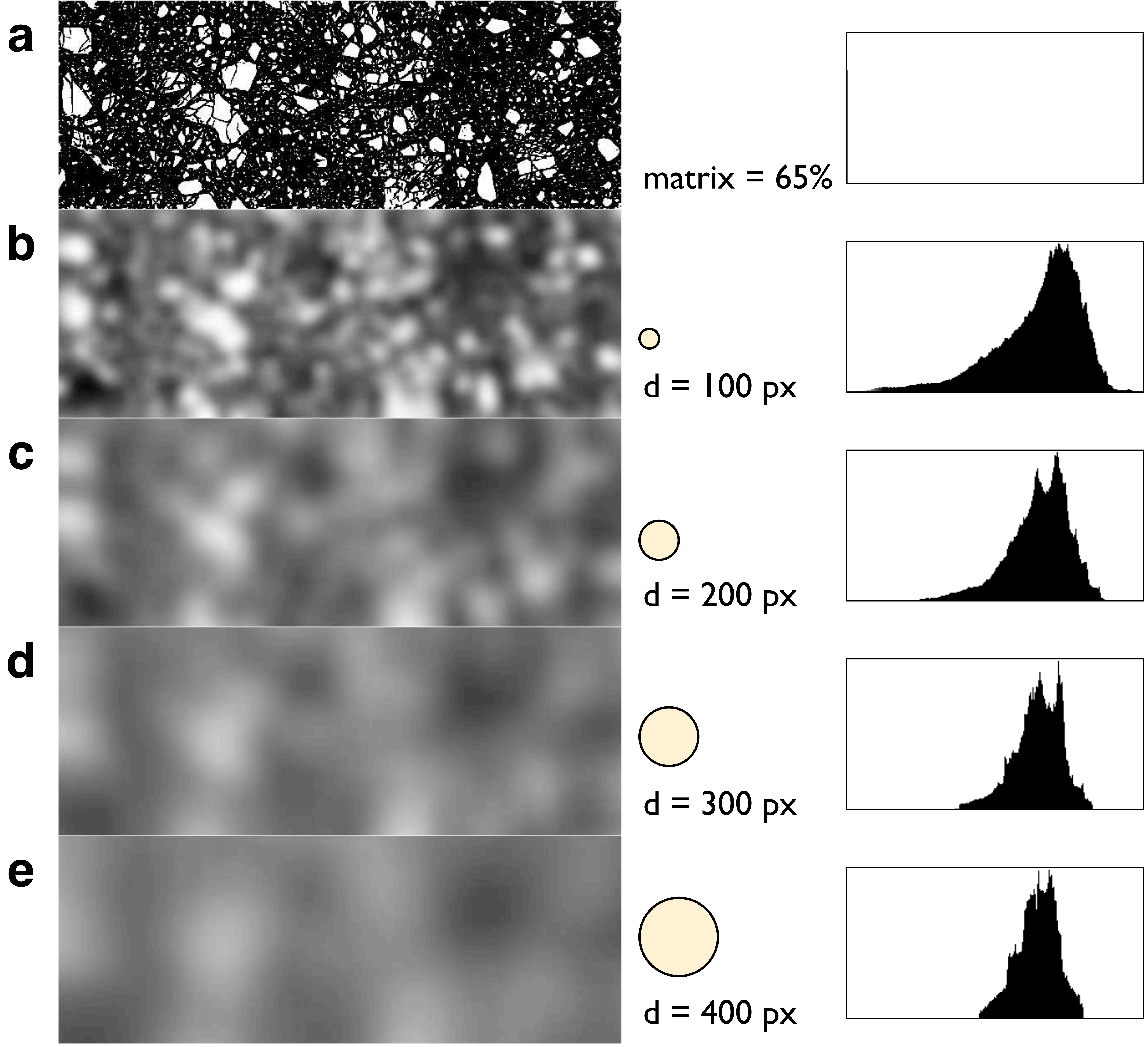

Figure 13.19
Creating matrix density maps by Gauss convolution..
Matrix density images are calculated by de-magnifying image proportional to 63 · 63 Gauss filter kernel (maximum filter size for Image SXM), (2) convolving, and (3) re-magnifying to original size.
(a) Original bitmap, average gray value = 164, corresponding to matrix density of 65 %;
(b) to (e) matrix density images, the corresponding filter diameters are indicated; note that range in histograms decreases while average matrix density remains constant (65 %).

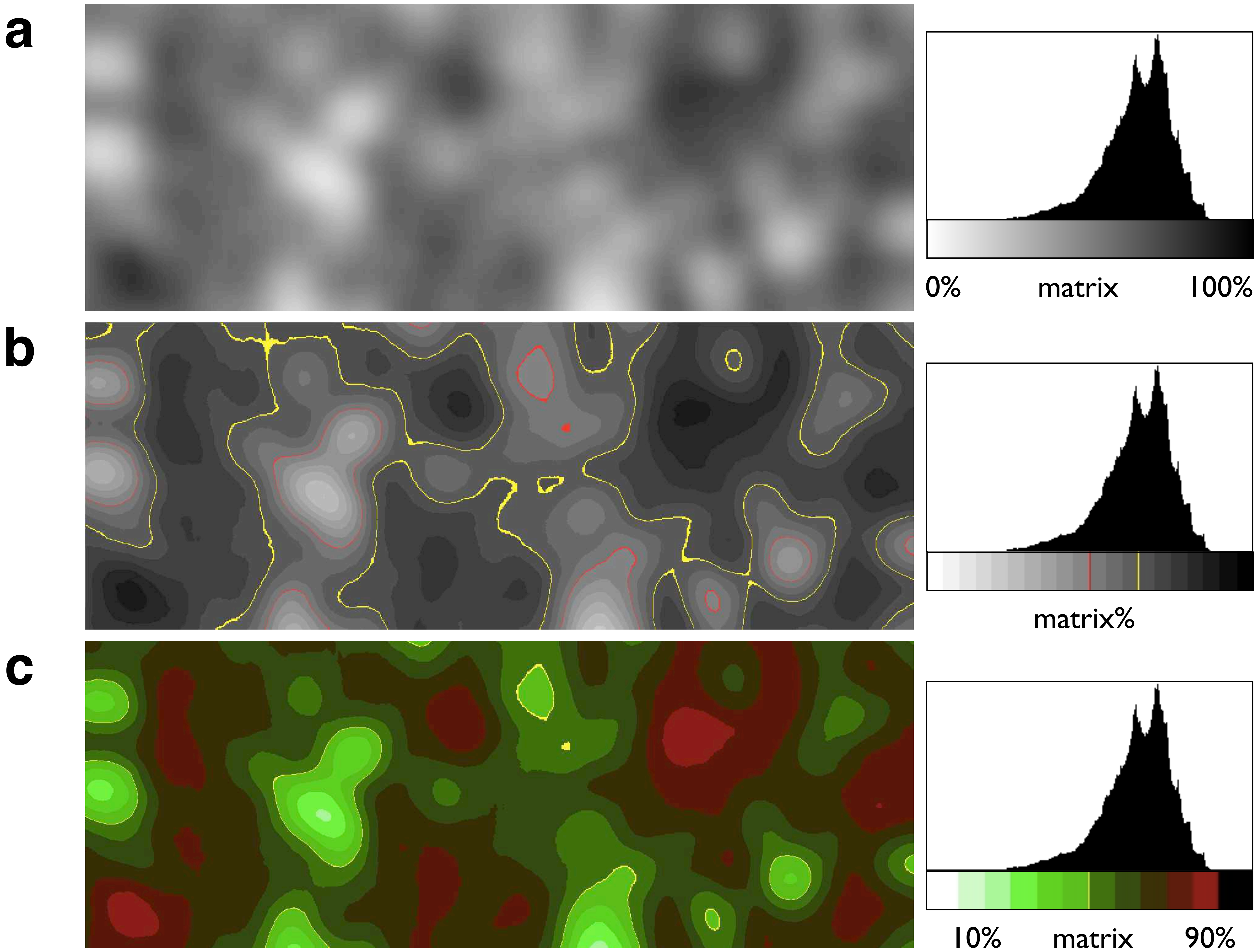

Figure 13.20
Visualizing matrix density maps.
(a) Scaled matrix density map, diameter of Gauss filter = 200 pixels;
(b) same as (a) seen with 20 gray levels, 50% and 65% contour are indicated in red and yellow, respectively;
(c) color coding of matrix content, lower cut-off = 10% (white), upper cut-off = 90% (black).

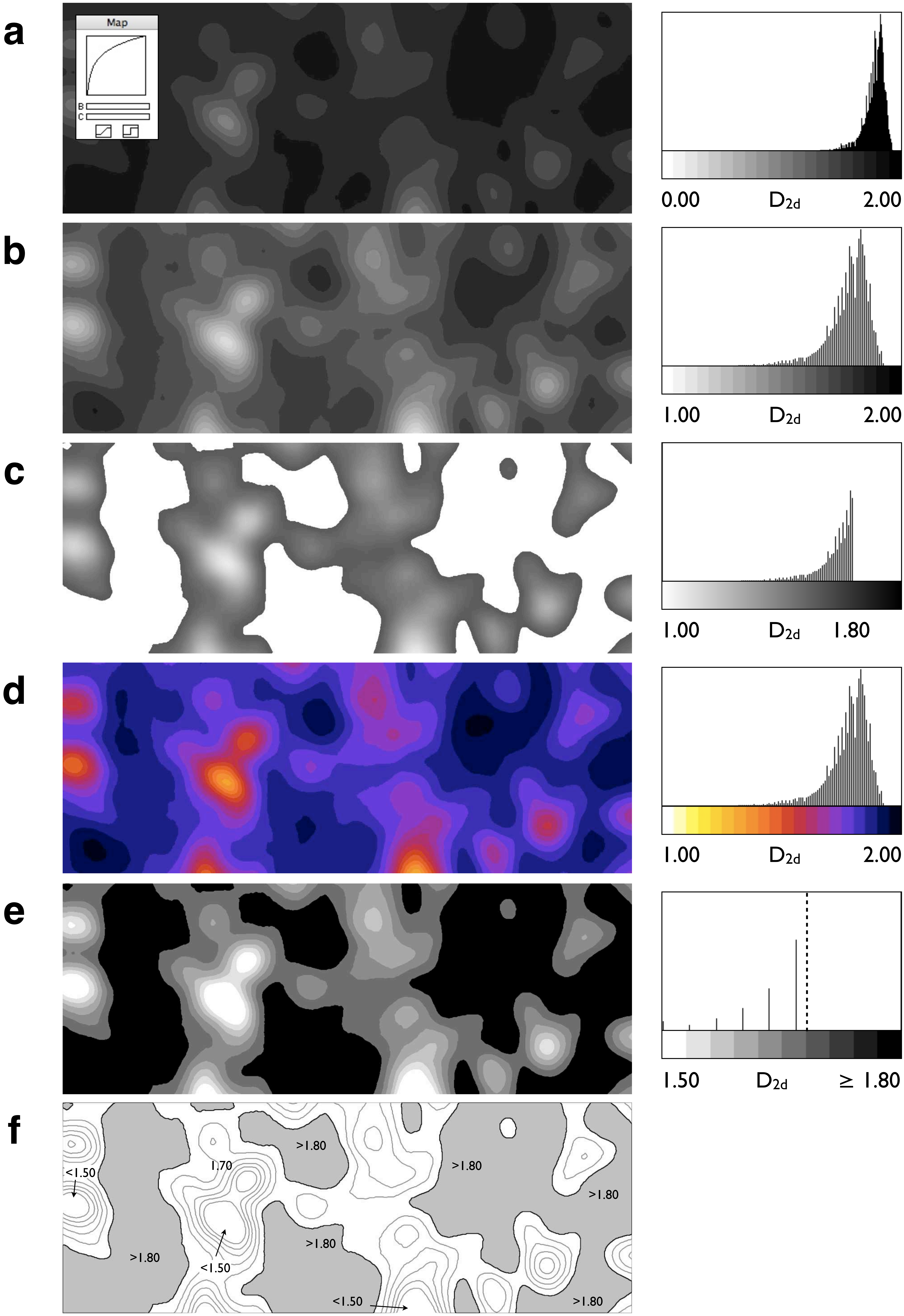

a
Map
B
C
0.00
D2d
2.00
b
1.00
D2d
2.00
c
1.00
D2d
1.80
d
1.00
D2d
2.00
e
1.50
D2d
≥ 1.80
f
>1.80
1.70
<1.50
>1.80
>1.80
>1.80
>1.80
<1.50
<1.50
>1.80

Figure 13.21
Converting matrix density to fractal dimension.
(a) Scaled map of fractal dimension (D map) obtained by applying LUT3 (for $L_m = 1/8$) to matrix density image (Gauss filter d = 200 pixels); average $D_{2d} = 1.76$; LUT shown in upper left corner;
(b) same as (a) after stretching gray values to ($1.00 < D_{2d} < 2.00$);
(c) same as (a) after cropping to $D_{2d} < 1.8$;
for comparison, (a) and (b) shown with 20 gray levels;
(d) same as (a) using 'Fire-2' LUT of Image SXM and setting LUT options to 20 colors;
(e) same as (c), after applying command [E] of the Lazy D map macro a second time ($1.50 \leq D_{2d} \leq 2.00$), filling the white area with black, setting LUT options to 10 colors and applying LUT;
(f) contour map obtained from (e) using 'Find Edges' command (Process menu).

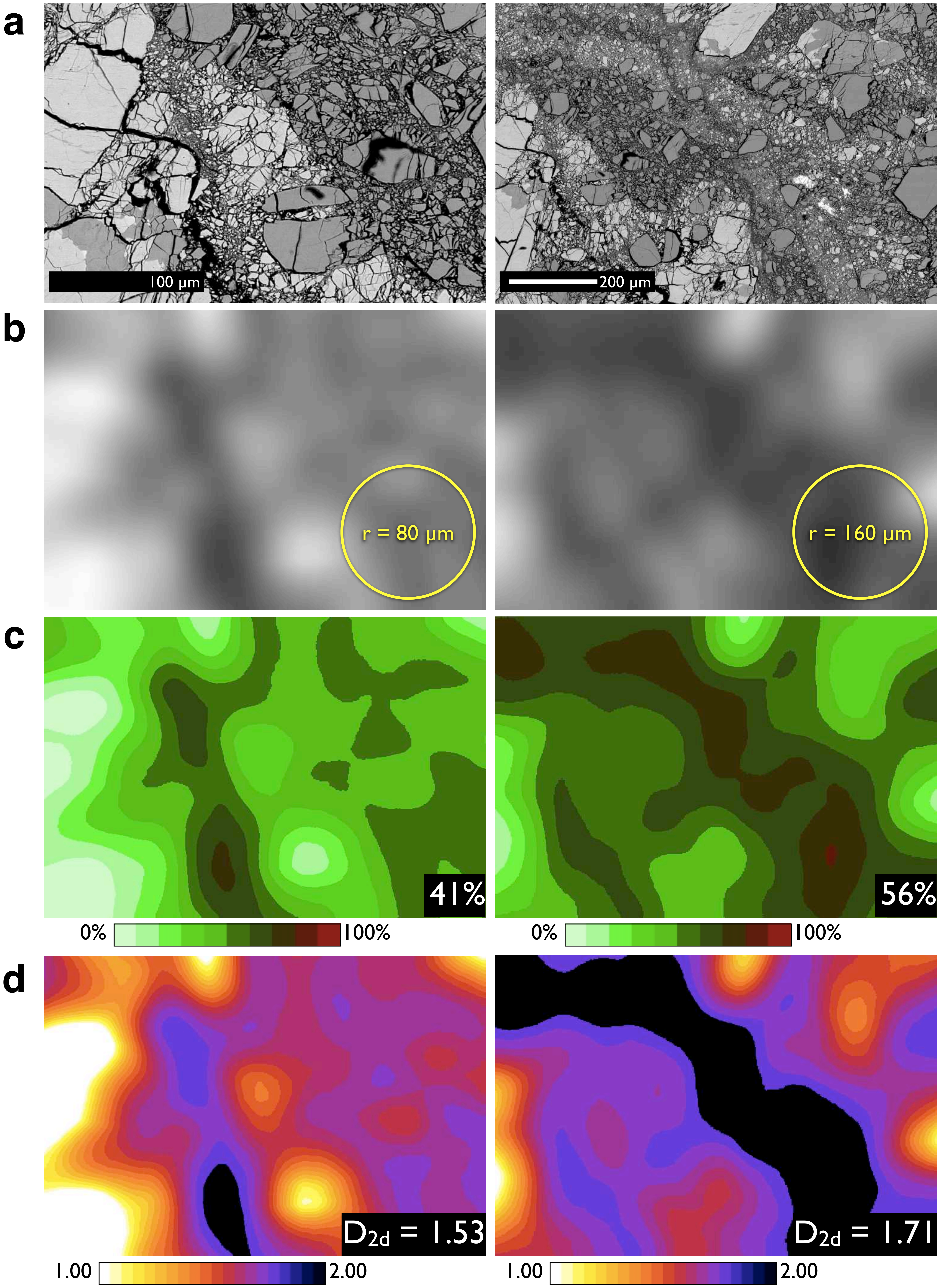

Figure 13.22
Two examples for D mapping. (a) SEM micrographs of experimentally produced fault at two different magnifications; (b) matrix density maps; size of Gauss filter is indicated by yellow circle; (c) color-coded matrix density maps; average matrix content is indicated; (d) D maps using LUT3 for a cut-off matrix grain size of L_m = 1/8; average fractal dimension, D_{2d}, of grain size distribution is indicated.

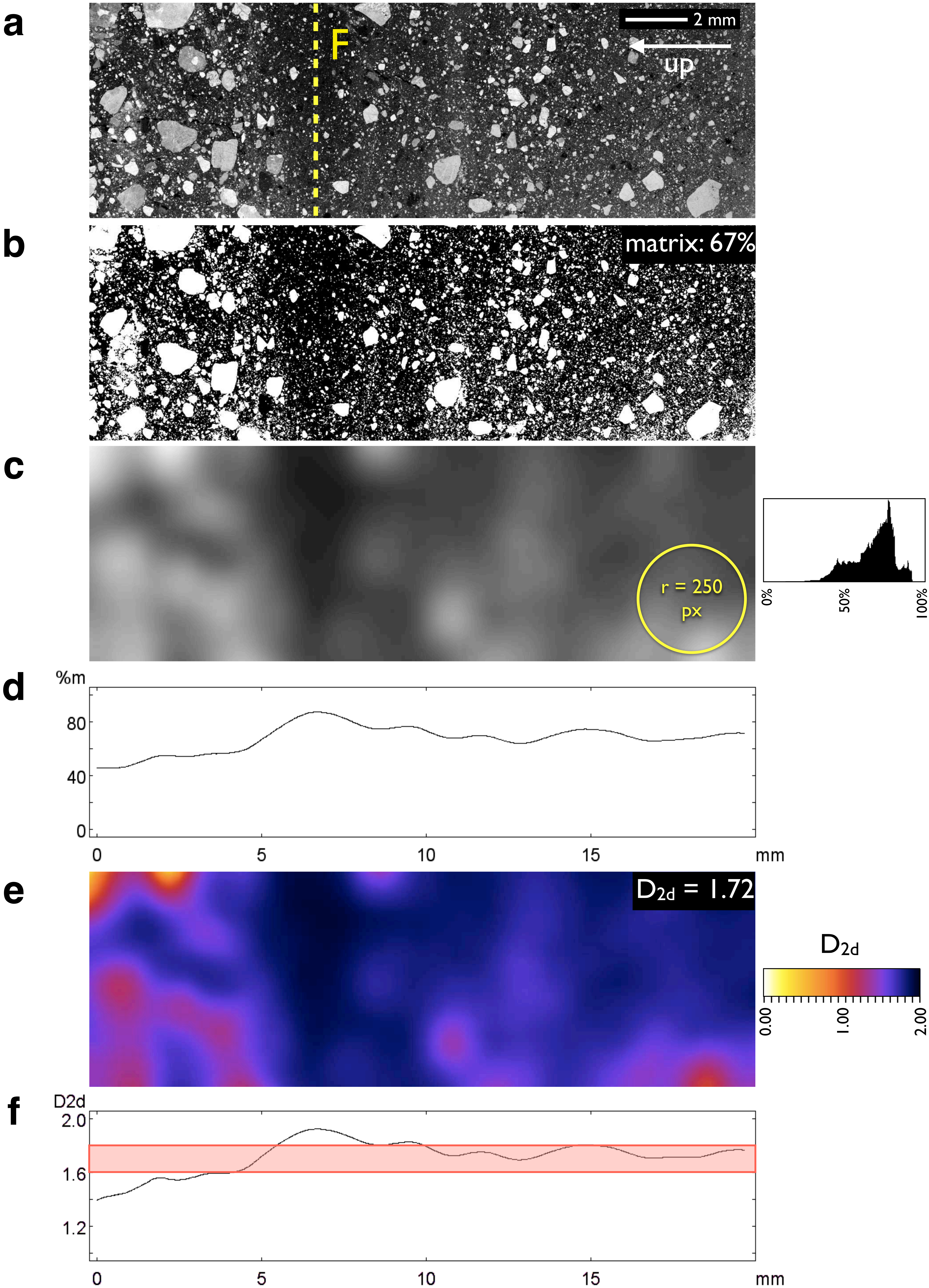
a
F
2 mm
up
b
matrix: 67%
c
r = 250 px
0%
50%
100%
d
%m
80
40
0
0
5
10
15
mm
e
D2d = 1.72
D2d
0.00
1.00
2.00
f
D2d
2.0
1.6
1.2
0
5
10
15
mm

Figure 13.23
D map of natural fault rock.
(a) Thin section of natural fault rock taken from low angle detachment fault, F = trace of (horizontal) fault surface;
(b) bitmap of (a); average density indicated;
(c) matrix density map; histogram on right; size of Gauss filter indicated by yellow circle;
(d) matrix density profile of (c), averaged over image height;
(e) D map of (c) using LUT2 (L_m = 1/4); color coding on right; average fractal dimension indicated;
(f) D profile of (e), averaged over image height; range of values ($1.60 \leq D_{2d} \leq 1.80$) is highlighted.